analytical chemistry

Article

pubs.acs.org/ac

Visualizing Breast Cancer Cell Proliferation and Invasion for Assessing Drug Efficacy with a Fluorescent Nanoprobe

Mingming Luan, Longhai Yu, Yanhua Li, Wei Pan, Xiaonan Gao, Xiuyan Wan, Na Li,* and Bo Tang*

College of Chemistry, Chemical Engineering and Materials Science, Collaborative Innovation Center of Functionalized Probes for Chemical Imaging in Universities of Shandong, Key Laboratory of Molecular and Nano Probes, Ministry of Education, Institute of Molecular and Nano Science, Shandong Normal University, Jinan, Shandong 250014, P. R. China

Supporting Information

ABSTRACT: Hard-to-treat cancers are closely relative to uncontrolled cell proliferation, invasion, and metastasis. Assessing proliferation and invasion properties of tumor cells both *in vitro* and *in vivo* is especially important for acquiring reliable information for cancer pathogenesis, drug screening, and therapeutic effect evaluation. Herein, we developed a multicolor fluorescent nanoprobe for simultaneously monitoring breast cancer cells' proliferation marker Ki-67 and invasion marker urokinase plasminogen activator (uPA). After treated with the anticancer drugs tamoxifen and curcumin, the changes in cancer cell proliferation and invasion properties were visually detected and therapeutic effects of corresponding drugs were further assessed *in vitro* and *in vivo*. The design of the fluorescent nanoprobe opens up an avenue for investigating unscheduled proliferation, invasion, and metastasis in living cells and *in vivo* and as such will be a promising tool to screen antitumor drugs and evaluate drug efficiency in an extremely efficient manner.

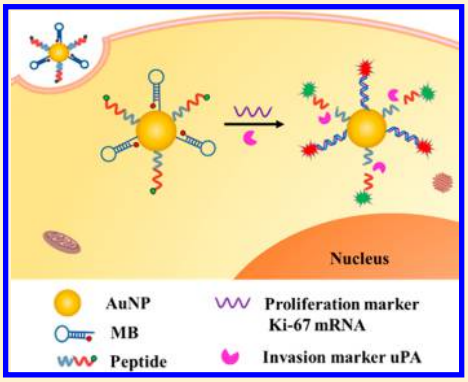

Cancer is a highly fatal disease characterized by many molecular genetic alterations involving deregulated proliferation,[1−4] invasion,[5−7] and metastasis.[8−10] Since the carcinogenic process usually relates with cell cycle dysfunction and endless proliferation, tumor cells frequently display uncontrolled proliferation accompanied by invasion and metastasis, which leads to new lesions.[11−14] Therefore, tremendous efforts have been focused on studying cell proliferation and invasion properties, which are pivotal to understand the carcinoma progression and assess the therapeutic effect in cancer therapies.[15,16] For instance, tumor-biological biomarkers reflecting cell proliferation and invasion are recommended clinical applications for evaluating cancer.[17] The common proliferation marker Ki-67, which is significantly overexpressed in cancer cells, has been used to predict the magnitude of chemotherapy benefit in breast cancer.[18,19] Moreover, the invasion marker urokinase plasminogen activator (uPA) implicated in cancer development is a significant predictive factor to investigate disease recurrence and invasive potential of cancer cells.[20,21] Therefore, studying cell proliferation and invasion significantly helps understanding cancer progress, assessing therapeutic response, and screening new anticancer drugs.[22−24]

At present, many biological techniques have been applied to evaluate cells proliferation and invasion. The BrdU immunohistochemistry,[25,26] Western blot (WB),[27] and reverse transcription-polymerase chain reaction (RT-PCR)[28,29] were traditional techniques based on biomarkers. However, such approaches require a large number of cell samples, substantial time, and complicated processes. Moreover, the cell lysates or organic solvents are used in these projects and the sample is measured directly in cell homogenates. Furthermore, certain biostatistical methods, including cell counting and transwell invasive assay, have the disadvantages of causing cells death besides time-consuming and tedious operation.[30−32] To the best of our knowledge, no approach has been employed to simultaneously investigate cell proliferation and invasion in living cells and *in vivo*. Therefore, it is imperative to develop a new strategy for detecting proliferative and invasive abilities of living cells for more comprehensive understanding of cancer occurrence and development, rapid and reliable antitumor drugs screening, and more accurate assessment of therapeutic effects.

Fluorescence image analysis provides stimulating opportunities to visually detect components in living cells and *in vivo* due to its excellent advantages of rapidity, damage free, and visual identification.[33−38] In this regard, a new multicolor fluorescent nanoprobe capable of simultaneously and visually detecting the proliferation marker Ki-67 mRNA and invasion marker uPA protein was designed and prepared (Scheme 1). The nanoprobe was prepared by immobilizing the synthetic DNA molecular beacons (MBs) and peptides on the gold nanoparticles (AuNPs), step-by-step via Au−S bond formation.[39,40] The MBs can identify Ki-67 mRNA, and the peptides can be specifically cleaved by uPA.[41] The multicolor nanoprobe

Received: August 5, 2017
Accepted: September 8, 2017
Published: September 8, 2017

DOI: 10.1021/acs.analchem.7b03146
Anal. Chem. 2017, 89, 10601−10607

Scheme 1. Schematic Illustration of the Nanoprobe for Detection of Intercellular Ki-67 mRNA and uPA

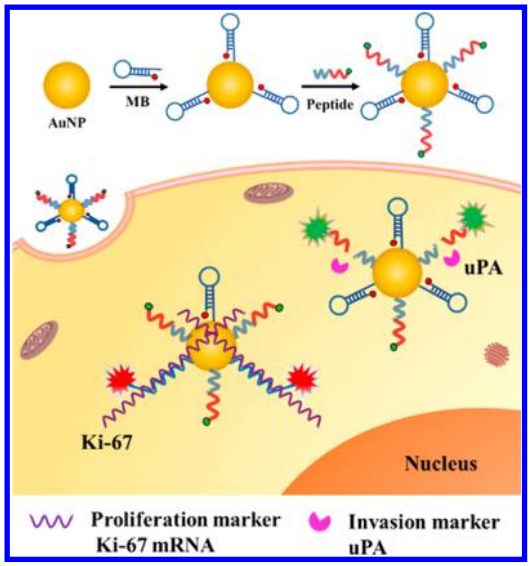

not only provides a new approach for the detection of proliferation and invasion in living cells and *in vivo* but also offers a faster and more efficient method for new anticancer drug screening and evaluating the drug effect.

EXPERIMENTAL SECTION

Preparation of the Nanoprobe. The MB (labeled with Cy5) was added to AuNPs solution (1 nM) with a final concentration of 50 nM and shaken for 4 h. SDS solution with 0.1% final concentration was further added to the mixture and rocked overnight. Phosphate buffered saline (PBS) (pH 7.4) containing 1 M NaCl was added to the mixture to yield 0.01 M of phosphate solution and 0.1 M of NaCl by 8 times addition with a 1 h interval. After aging for 2 days at room temperature, the resulting solution was centrifuged (13000 rpm, 0.5 h) at 4 °C to remove the excess MB and resuspended in PBS for three times, and last the peptide at a final concentration of 1500 nM was added to the above solution (1 nM). The mixture was stirred tenderly for 2 days. The solution was then centrifuged (10000 rpm, 20 min) at 4 °C and resuspended in PBS for three times. Finally the nanoprobe was dispersed in PBS and stored at 4 °C in the dark. The concentration of AuNPs was calculated by the intensity of their extinction wavelength at 524 nm (ε = 2.7 × 10^8 L mol^{-1} cm^{-1}).

Target Recognition and Specificity of Nanoprobe. For multiplexed detection of analytes, the nanoprobe (1 nM) was incubated with the complementary Ki-67 DNA target and uPA target, respectively, with increasing DNA targets concentrations (0, 10, 20, 30, 40, 50, 60, 70, 90, 100, 150, 200 nM) or uPA concentration (10^{-4}, 10^{-3}, 10^{-2}, 10^{-1}, 0.2, 0.3, 0.4 μg/mL). After incubation at 37 °C for 1 h, the fluorescence intensity was acquired at corresponding excitation wavelengths. To study the targeting specificity of nanoprobe, the precisely matched Ki-67 DNA target (200 nM), uPA (0.4 μg/mL) for MB or peptide and other targets were added to the nanoprobe (1 nM) for 1 h at 37 °C. The fluorescence intensity of the nanoprobe was recorded. All experiments were repeated at least three times.

Kinetics Experiment. The nanoprobe solution was incubated with Ki-67 DNA target (200 nM) and uPA (0.4 μg/mL) at 37 °C, respectively, and the fluorescence was monitored with increasing time (0, 5, 10, 15, 20, 30, 40, 50, 60 min or 0, 5, 10, 15, 20, 25, 30, 35, 40, 45, 50, 55, 60 min). The fluorescence of Cy5 and RhB was recorded at their corresponding excitation and emission wavelengths.

Confocal Fluorescence Imaging. In confocal fluorescence imaging experiments of different breast cell types, the normal mammary MCF-10A cells, weakly invasive MCF-7 cells, and highly invasive MDA-MB-231 cells were seeded on chamber slides and incubated for 24 h. Then the cells were incubated with the DMEM medium containing the nanoprobe (1 nM) for 4 h at 37 °C. The cells were thoroughly washed with PBS and then imaged by confocal laser scanning microscopy (CLSM) with 543 and 633 nm excitation.

For the medium's effect obtained from cancer cells on the proliferation and invasion of normal cells, the medium in which MDA-MB-231 cells had been cultured for 2 days and collected for centrifugation. MCF-10A cells were divided into four groups and grown in the conditioned medium, which is a mixture of equal amounts MDA-MB-231 medium and fresh DMEM medium for 0, 3, 6, 9 days, respectively. Then the nanoprobe (1 nM) was added to the four groups of MCF-10A cells, and 4 h later the fluorescence images of cells were captured using the 543 nm laser and 633 nm laser.

The drugs' influence on the proliferation and invasion of cancer cells was evaluated by lowly invasive MCF-7 cells (parallel groups). Groups I was cultured in DMEM medium alone serving as the control; Group II was treated with β-estradiol (10 nM); Group III was treated with tamoxifen (2.5 μM); and Group IV was treated with curcumin (10 μM) for 4 days, respectively. The four groups of cells were incubated with 1 nM nanoprobe for 4 h at 37 °C and then examined by CLSM. In another experiment, highly invasive MDA-MB-231 cells were divided into three groups. One group was treated with tamoxifen (2.5 μM) and the other group was treated with curcumin (10 μM) for 4 days. The cells without treatment served as the control. The subsequent steps were performed as described above using 1 nM nanoprobe, and finally the CLSM images of MDA-MB-231 cells were obtained under 543 and 633 nm excitation.

Direct Cell Counting. Cells were resuspended in DMEM and seeded at a density of 5 × 10^3 cells per well in 24-well plates. Cells were grown for 7 days and counted in triplicates daily to produce a time-dependent growth curve. The cells were counted in Neubauer-counting chamber.

CCK-8 Assay. Cells were resuspended in DMEM and plated at a density of 2 × 10^3 cells per well in 96-well plates. In the CCK-8 assays of different breast cell types, MCF-10A, MCF-7, and MDA-MB-231 cells were cultured in three replicate filters for 7 days and relative cell growth was determined by a CCK-8 kit (Biosharp). The optical density (OD) values at 450 nm were detected using a microplate reader with BioTek Synergy 2. The cancer cells medium's influence on normal cells and the drugs upon cells were evaluated: cells were plated in 96 well multiwell plates and further treated with conditional medium or different drugs as described in the CLSM experiment. Finally, the OD values of treated cells were measured at 450 nm.

Animal Imaging. All animal experiments were managed under the Principles of Laboratory Animal Care (Peoplés Republic of China). For murine tumor xenograft experiments, MDA-MB-231 cancer cells (2 × 10^6 cells) were injected subcutaneously into the right flank of female nude mice (~20 g, 4−6 weeks). When the tumors' diameter reached approximately 5 mm, the mice were randomly divided into three

DOI: 10.1021/acs.analchem.7b03146
Anal. Chem. 2017, 89, 10601−10607

groups. Two groups were treated with of curcumin and tamoxifen via intraperitoneal (ip) injection, respectively. The concentrations of two drugs are 0.1 g/kg each and dissolved in 10% DMSO. The group received ip injection of equal volume of vehicle (DMSO) diluted in PBS served as the control group. Three other groups of mice were injected once daily, and 4 days later, the nude mice were injected intratumorally with the nanoprobe (100 nM, 50 μL) for 4 h. The mice were then anesthetized with chloral hydrate and imaged for fluorescence using the IVIS Lumina III imaging system with 540 nm excitation (RhB) for Ki-67 mRNA detection and 620 nm excitation (Cy5) for uPA detection, respectively. Ki-67 and uPA staining were carried out at 4 days post-treatment.

RESULTS AND DISCUSSION

Preparation and Characterization of the Nanoprobe. The nanoprobe was synthesized using 20 nm citrate-capped AuNPs with effective quenching efficiency, which was suitable for accommodating more recognition units.[42] AuNPs were successively modified with MB and peptide by the formation of Au−S bonds. High-resolution transmission electron microscopy (HRTEM) images (Figure S1) show that the AuNPs and the nanoprobe display spherical morphology with an average size of 20 nm. The nanoprobe was characterized by UV−vis spectroscopy (Figure S2), and the red shift of the maximum absorption from 519 to 524 nm indicates that the AuNPs were successfully functionalized with MB and peptide. According to the previous literature, each AuNP was calculated to carry 36 ± 1 Cy5 labeled MB targeting Ki-67 mRNA and 74 ± 1 RhB labeled peptide targeting uPA (Figure S3).

***In Vitro* Studies of the Nanoprobe.** To test the capability of the nanoprobe for simultaneously detecting the DNA targets and uPA targets, the fluorescence responses of the nanoprobe to respective targets were examined. As shown in Figure 1A, the

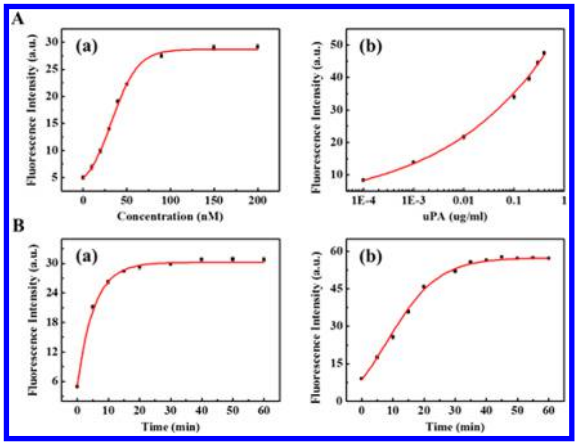

Figure 1. Fluorescence recovery (A) and kinetic studies (B) of the nanoprobe in the presence of Ki-67 targets (a) and uPA targets (b) measured with 648 and 554 nm excitation wavelengths, respectively. In kinetic studies, the concentrations of Ki-67 and uPA targets are 200 nM and 0.4 μg/mL, respectively.

fluorescence recoveries were observed by addition of the synthetic targets in a concentration-dependent manner, which suggested that the nanoprobe could signal the presence of specific targets. The kinetic profiles of the nanoprobe toward two different targets were further performed (Figure 1B). The nanoprobe could respond quickly to the perfectly complementary DNA targets within 10 min and uPA targets within 30 min. The selectivity of the nanoprobe was also examined to reveal the nanoprobe generation of high fluorescence signal upon meeting the perfectly matched DNA targets or uPA targets. In addition, high specificity was also acquired through comparing with other targets (Figure S4). The results indicated that the nanoprobe could be applied in simultaneously monitoring the two types of targets in living cells.

MTT Assay. The cell toxicity of the nanoprobe was evaluated by MTT assay in MCF-10A, MCF-7, and MDA-MB-231 cells. As shown in Figure S5, the cell viabilities of three breast cell lines were all over 90% after incubation with free AuNPs and nanoprobe for various times, which demonstrated that the nanoprobe exhibited almost no cytotoxicity and could be applied in the detection of intracellular biomolecules.

Intracellular Imaging of the Nanoprobe. The multicolor nanoprobe was then applied to investigate cell proliferation and invasion by monitoring the relative fluorescence of marker Ki-67 and uPA in living cells, respectively. Three different human breast cell lines were selected: normal MCF-10A mammary epithelial cells, weakly invasive MCF-7 breast cancer cells, and highly invasive MDA-MB-231 breast cancer cells. Proliferative marker Ki-67 expressions in many malignant tumors including breast, lung, and stomach cancers are significantly higher than that in normal cells. Moreover, invasive marker uPA is expressed at higher levels in malignant tumors than different normal and cancerous tissue. The expressions of Ki-67 and uPA are related with the prognosis in patients. After incubation of the three breast cancer cell lines with a 1 nM nanoprobe for 4 h, a red fluorescent signal for Ki-67 mRNA and a green fluorescent signal for uPA were examined under CLSM. In Figure 2A, the two fluorescent signals were the weakest in MCF-10A cells and the strongest in MDA-MB-231 cells. The

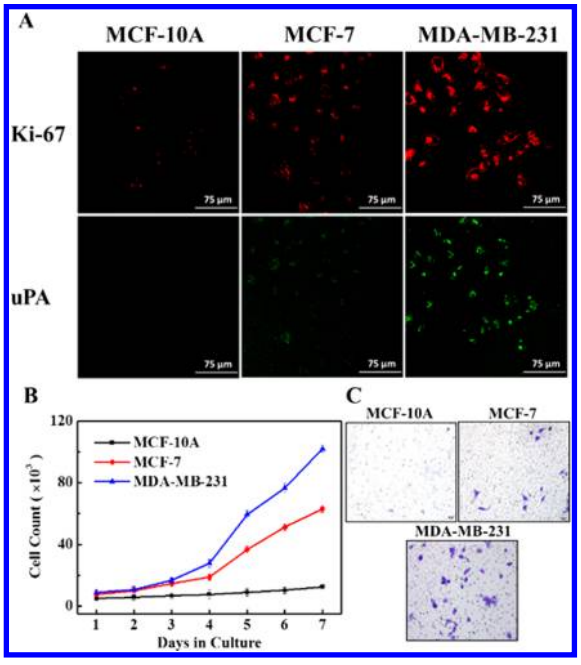

Figure 2. (A) Intracellular imaging of Ki-67 mRNA and uPA in MCF-10A, MCF-7, and MDA-MB-231 cells under CLSM. The cells were incubated with the nanoprobe (1 nM) for 4 h at 37 °C. The two channels were recorded with the excitation of 633 and 543 nm, respectively. Scale bars: 75 μm. (B) Cell growth curve analysis obtained by counting cell numbers daily in triplicates. (C) Transwell invasion assay for three breast cell lines.

DOI: 10.1021/acs.analchem.7b03146
Anal. Chem. 2017, 89, 10601−10607

fluorescence signals, by contrast, were moderate in MCF-7 cells. These results demonstrated that the strong-to-weak sequences of the relative levels of two biomarkers were MDA-MB-231, MCF-7, and MCF-10A, and with the increase order of the relative proliferation and invasion capabilities. The results of RT-PCR and WB revealed the relative expressions of Ki-67 mRNA and uPA in MCF-7 cells were all higher than that in MCF-10A but lower than that in MDA-MB-231 cells (Figures S6 and S7). The results exhibited consistency with the CLSM results, which further indicated that the relative levels of the two markers could be reflected by fluorescence intensities. To test cellular proliferation of the three breast cancer cell lines, cell growth curves and CCK-8 assays were studied (Figure 2B and Figure S8). Compared with MCF-7 cells, the growth speed was increased in MDA-MB-231 cells and decreased in MCF-10A cells, which demonstrated that the strengths of proliferative potential were MDA-MB-231 > MCF-7 > MCF-10A. To measure cell invasiveness potential, transwell invasion assays were then performed (Figure 2C). Similar to the proliferative properties, MDA-MB-231 cells exhibited the strongest invasive capabilities among the three cell types. These results were consistent with imaging studies, which implies that the designed fluorescent nanoprobe can be useful for simultaneously visualizing proliferation and invasiveness in living cells.

Next, the multicolor nanoprobe was investigated on the proliferation and invasion of normal cells affected by cancer cells. Normal MCF-10A cells were separated into four groups in parallel, which were incubated with highly invasive MDA-MB-231 cancer cell culture medium for 0, 3, 6, 9 days, respectively. The results from RT-PCR and WB indicate that the relative levels of Ki-67 mRNA and uPA in MDA-MB-231 medium cultured MCF-10A cells kept increasing with cumulative incubation time (Figures S9 and S10). Four groups of normal cells cultured with MDA-MB-231 medium were treated with nanoprobe and imaged by CLSM. As shown in Figure 3A, the time-related increase of the red and green fluorescence signals in MCF-10A cells was observed, demonstrating that the expressions of Ki-67 mRNA and uPA increased consistently with the results of PCR and WB. The results implied that proliferative and invasive properties of normal cells were enhanced when MCF-10A cells were influenced by MDA-MB-231 medium. Afterward, the influence on normal cells via cancer cells was further evaluated. As demonstrated in Figure 3B, cell proliferation was first estimated by the CCK-8 kit and the stronger proliferative potential was associated with longer incubation time. The CFSE staining was also applied to analyze cell proliferation (Figure S11). During the same incubation time, the percentage of R3 area in the cell group treated with MDA-MB-231 medium was higher than that in the untreated cells, which specified that the proliferation of MCF-10A cells could be enhanced after incubation with MDA-MB-231 medium. Finally, transwell invasion assays were performed to assess invasive potential. Similar to proliferative properties, the invasiveness of MCF-10A cells was gradually promoted with increasing incubation time (Figure 3C). All these results strongly support that the nanoprobe detects the changes in proliferative and invasive potencies of normal cells affected by cancer cells.

Since evaluating of cell proliferation and invasion in cancer cells helps predict anticancer drug efficacy, the therapeutic response was assessed through detecting cell proliferation and invasion with the nanoprobe. The poorly invasive MCF-7 cells

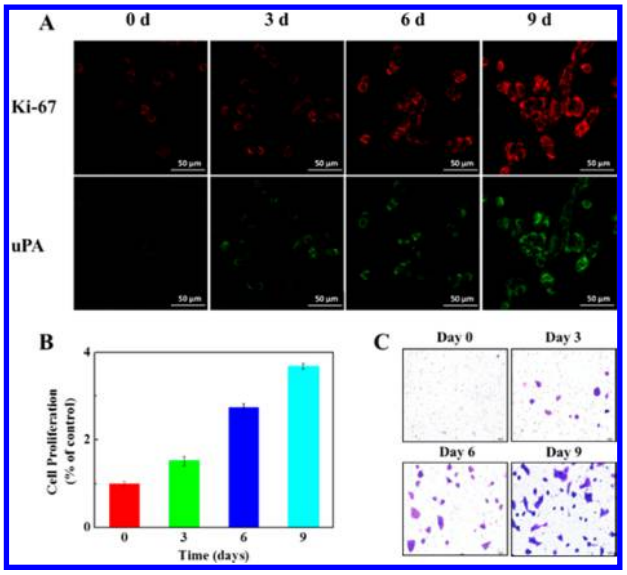

Figure 3. (A) Intracellular imaging of Ki-67 mRNA and uPA in MCF-10A cells treated with MDA-MB-231 medium for 0, 3, 6, 9 days, respectively. Scale bars: 50 μm. (B) Evaluation of cell proliferation by CCK-8 assay in MCF-10A cells treated with MDA-MB-231 medium. Values are shown as mean ± SD of three distinct experiments. (C) Effects of the medium from MDA-MB-231 cells on MCF-10A cells invasion.

were chosen and divided into four groups. Since β-estradiol stimulates cell proliferation and tamoxifen and curcumin are current anticancer drugs for breast cancer,[43−45] three groups of cells were treated with each, respectively, and the untreated group served as control. Therefore, four groups of cells were incubated with the nanoprobe and imaged by CLSM. As shown in Figure 4A, the red fluorescent signals increased after β-estradiol treatment but decreased after tamoxifen and curcumin treatment compared with the control group. However, the

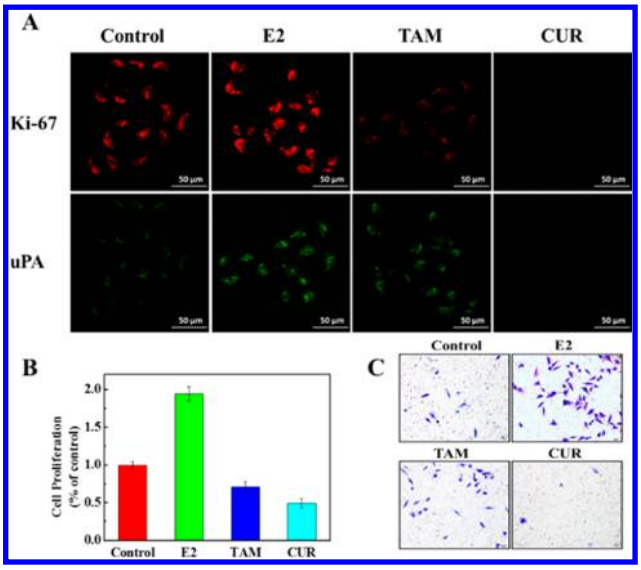

Figure 4. (A) Confocal fluorescence images of different levels of Ki-67 mRNA and uPA in MCF-7 cells. Scale bars: 50 μm. (B) Evaluation of cell proliferation by CCK-8 assay. (C) Transwell invasion assay. (A–C) MCF-7 cells were treated with β-estradiol (E2, 10 nM), tamoxifen (TAM, 2.5 μM), and curcumin (CUR, 10 μM), respectively, and the untreated group served as the control.

DOI: 10.1021/acs.analchem.7b03146
Anal. Chem. 2017, 89, 10601−10607

green fluorescent signals increased with β-estradiol and tamoxifen treatment but decreased with curcumin treatment. Hence, the proliferation and invasion were enhanced by β-estradiol but suppressed by curcumin. While, interestingly, tamoxifen inhibited cell proliferation but promoted cell invasion. The CLSM results were further verified by the assays as described above. The expression levels of Ki-67 and uPA were in agreement with PCR and WB results (Figures S12 and S13). The CCK-8 analysis indicated that proliferation was increased by β-estradiol and decreased by tamoxifen and curcumin consistent with the results of CFSE-based proliferation assays (Figure 4B and Figure S14). The invasive capabilities were further evaluated by counting the invasive cells (Figure 4C). The changes in invasion were similar to the changes in proliferation after β-estradiol and curcumin treatment. Instead, the invasion was induced with tamoxifen treatment. These results are in agreement with the imaging results, suggesting that the proliferation and invasiveness of cancer cells treated with anticancer drug could be monitored with the nanoprobe.

For the next step, the proliferation change was investigated as contrary to invasion change in highly invasive MDA-MB-231 cells treated with tamoxifen and curcumin. MDA-MB-231 cells were divided into three groups, the untreated group was set as control, and two other groups of cells were treated with tamoxifen and curcumin under the same conditions as those used in MCF-7 cells, respectively. The three groups of cells were incubated with the nanoprobe afterward. In Figure 5A, the red and green fluorescent intensities were decreased in curcumin-treated cells compared with untreated cells, which indicated the levels of two biomarkers were inhibited by curcumin. Unlike curcumin, the two fluorescent intensities had little change in tamoxifen-treated cells indicating tamoxifen had a minimal effect on the two biomarkers levels. These results showed that curcumin could efficiently inhibit the proliferation and invasion of MDA-MB-231 cells while tamoxifen had an unobvious effect on MDA-MB-231 cells. In addition, the relative assays as stated above were performed and the expression changes of Ki-67 and uPA were confirmed by PCR and WB results (Figures S15 and S16). The CCK-8 tests indicated that curcumin significantly inhibited proliferation of MDA-MB-231 cells but tamoxifen had a minimal effect on cell proliferation (Figure 5B), which was further verified by CFSE assays. The CFSE results implied that tamoxifen had little influence on proliferative potential but curcumin restrained this potential (Figure S17). The changes in invasion were similar to proliferation of MDA-MB-231 cells after being treated with the two drugs (Figure 5C). The evaluation of proliferation and invasion properties is consistent with the imaging results which reveal that the two properties of highly aggressive cancer cells are also detected with the nanoprobes. These results indicate the effects of tamoxifen and curcumin on proliferation and invasion in two breast cancer cells are different, which will lead to different therapeutic efficacy.

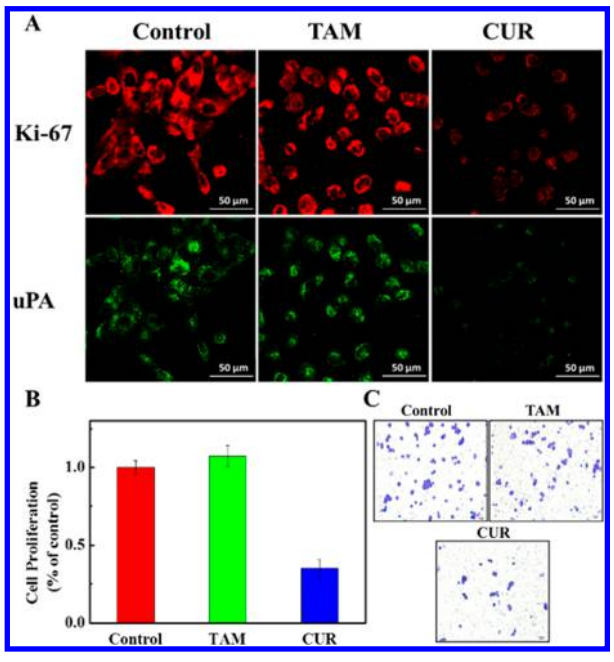

Figure 5. (A) Confocal fluorescence images of different levels of Ki-67 mRNA and uPA in MDA-MB-231 cells. Scale bars: 50 μm. (B) Evaluation of cell proliferation by CCK-8 assay. (C) Transwell invasion assay. (A–C) MDA-MB-231 cells were treated with TAM (2.5 μM) and CUR (10 μM), respectively.

***In Vivo* Fluorescence Imaging.** To evaluate the feasibility of nanoprobe for detecting Ki-67 mRNA and uPA *in vivo*, the xenograft mouse models with MDA-MB-231 cells were injected with the nanoprobe after the mice were treated with tamoxifen and curcumin. The fluorescent imaging of tumor region *in vivo* was performed with proper excitation (Figure 6). Compared to

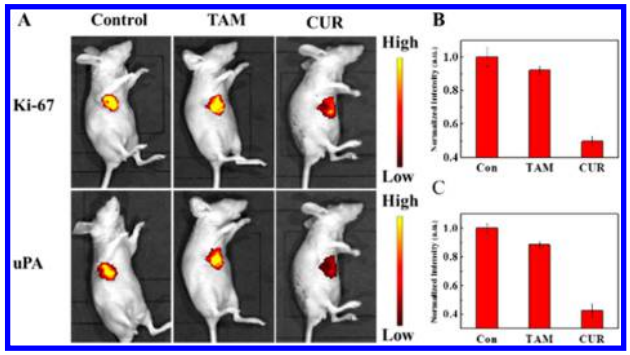

Figure 6. *In vivo* fluorescence images of mice bearing MDA-MB-231 tumors. (A) The excitation filter was 620 nm for Ki-67 mRNA and 540 nm for uPA. (B, C) Quantification of fluorescence intensity from Ki-67 and uPA. The mice were treated with TAM and CUR via ip injection, respectively; the DMSO-treated mice served as the control. All data were shown as mean ± SD, n = 3 per group.

the DMSO-treated mice, the curcumin-treated mice exhibited lower fluorescent signals for Ki-67 mRNA and uPA and tamoxifen-treated mice displayed comparative fluorescent signals, indicating that curcumin is effective treatment for MDA-MB-231 tumor while tamoxifen has a minute effect. Furthermore, the Ki-67 and uPA levels in tumor cells were checked by tumor sections using immunohistochemisty (Figure S18). The levels of the two markers were decreased in curcumin-treated group and had no remarkable changes in the tamoxifen-treated group compared to the control group. These results confirm that *in vivo* imaging of Ki-67 and uPA studies validates the nanoprobe with a reliable and convenient way to screen antitumor drugs and assess therapeutic effects.

CONCLUSIONS

In summary, a multicolor fluorescent nanoprobe based on AuNPs was designed and synthesized, which can be used to

DOI: 10.1021/acs.analchem.7b03146
Anal. Chem. 2017, 89, 10601–10607

simultaneously image proliferative marker Ki-67 mRNA and invasive marker uPA in living cells. The nanoprobe possesses remarkable specificity, rapid response, and favorable biocompatibility. Live-cell imaging revealed that the differences in efficacy existed between tamoxifen and curcumin due to the different influence of drugs on proliferation and invasiveness of cancer cells, which was further ascertained by *in vivo* imaging. Compared to traditional approaches for biomarker detection, the nanoprobe can simultaneously visualize the proliferative and invasive abilities *in vitro* and *in vivo*. More importantly, the nanoprobe can be used to evaluate the therapeutic efficacy of anticancer drugs. We envision that the current work has exciting potential applications as a platform for predicting drug therapy and guiding drug selection.

■ ASSOCIATED CONTENT

Supporting Information

The Supporting Information is available free of charge on the ACS Publications website at DOI: 10.1021/acs.analchem.7b03146.

Additional experimental details, DNA sequences and peptide information, TEM images, UV−Vis spectra, calibration curves, specificity of the nanoprobe against certain DNA targets and protein target, growth inhibition assay, detection of the Ki-67 mRNA levels by RT-PCR in MCF-10A, MCF-7, and MDA-MB-231 cells, Western blot analysis of uPA in MCF-10A, MCF-7 and MDA-MB-231 cells, *in vitro* cell growth analysis by CCK-8 assay in MCF-10A, MCF-7 and MDA-MB-231 cells, detection of the Ki-67 mRNA levels by RT-PCR in MCF-10A cells treated with MDA-MB-231 medium, and Western blot analysis of uPA in MCF-10A cells treated with MDA-MB-231 medium (PDF)

■ AUTHOR INFORMATION

Corresponding Authors

*Fax: (86)-531-86180017. E-mail: lina@sdnu.edu.cn.
*Fax: (86)-531-86180017. E-mail: tangb@sdnu.edu.cn.

ORCID

Bo Tang: 0000-0002-8712-7025

Notes

The authors declare no competing financial interest.

■ ACKNOWLEDGMENTS

This work was supported by 973 Program (Grant 2013CB933800), National Natural Science Foundation of China (Grants 21390411, 21535004, 21422505, 21375081, and 21505087), and Natural Science Foundation for Distinguished Young Scholars of Shandong Province (Grant JQ201503).

■ REFERENCES

(1) Jeggo, P. A.; Pearl, L. H.; Carr, A. M. *Nat. Rev. Cancer* **2016**, *16*, 35−42.
(2) Schulze, A.; Harris, A. L. *Nature* **2012**, *491*, 364−373.
(3) Hartwell, L. H.; Kastan, M. B. *Science* **1994**, *266*, 1821−1828.
(4) Hanahan, D.; Weinberg, R. A. *Cell* **2011**, *144*, 646−674.
(5) Hahn, W. C.; Weinberg, R. A. *N. Engl. J. Med.* **2002**, *347*, 1593−1603.
(6) Slattum, G. M.; Rosenblatt, J. *Nat. Rev. Cancer* **2014**, *14*, 495−501.
(7) Friedl, P.; Alexander, S. *Cell* **2011**, *147*, 992−1009.
(8) Chaffer, C. L.; Weinberg, R. A. *Science* **2011**, *331*, 1559−1564.
(9) Gupta, G. P.; Massague, J. *Cell* **2006**, *127*, 679−695.
(10) Hsieh, A. C.; Liu, Y.; Edlind, M. P.; Ingolia, N. T.; Janes, M. R.; Sher, A.; Shi, E. Y.; Stumpf, C. R.; Christensen, C.; Bonham, M. J.; Wang, S.; Ren, P.; Martin, M.; Jessen, K.; Feldman, M. E.; Weissman, J. S.; Shokat, K. M.; Rommel, C.; Ruggero, D. *Nature* **2012**, *485*, 55−61.
(11) Evan, G. I.; Vousden, K. H. *Nature* **2001**, *411*, 342−348.
(12) Marino-Enriquez, A.; Fletcher, C. D. *Nat. Rev. Cancer* **2014**, *14*, 701−702.
(13) Knoll, J. D.; Turro, C. *Coord. Chem. Rev.* **2015**, *282*−*283*, 110−126.
(14) Valastyan, S.; Weinberg, R. A. *Cell* **2011**, *147*, 275−292.
(15) Bonanni, B.; Puntoni, M.; Cazzaniga, M.; Pruneri, G.; Serrano, D.; Guerrieri-Gonzaga, A.; Gennari, A.; Trabacca, M. S.; Galimberti, V.; Veronesi, P.; Johansson, H.; Aristarco, V.; Bassi, F.; Luini, A.; Lazzeroni, M.; Varricchio, C.; Viale, G.; Bruzzi, P.; Decensi, A. *J. Clin. Oncol.* **2012**, *30*, 2593−2600.
(16) Anastas, J. N.; Moon, R. T. *Nat. Rev. Cancer* **2013**, *13*, 11−26.
(17) Harris, L.; Fritsche, H.; Mennel, R.; Norton, L.; Ravdin, P.; Taube, S.; Somerfield, M. R.; Hayes, D. F.; Bast, R. C. *J. Clin. Oncol.* **2007**, *25*, 5287−5312.
(18) Hoster, E.; Rosenwald, A.; Berger, F.; Bernd, H. W.; Hartmann, S.; Loddenkemper, C.; Barth, T. F.; Brousse, N.; Pileri, S.; Rymkiewicz, G.; Kodet, R.; Stilgenbauer, S.; Forstpointner, R.; Thieblemont, C.; Hallek, M.; Coiffier, B.; Vehling-Kaiser, U.; Bouabdallah, R.; Kanz, L.; Pfreundschuh, M.; Schmidt, C.; Ribrag, V.; Hiddemann, W.; Unterhalt, M.; Kluin-Nelemans, J. C.; Hermine, O.; Dreyling, M. H.; Klapper, W. *J. Clin. Oncol.* **2016**, *34*, 1386−1394.
(19) Cheang, M. C.; Chia, S. K.; Voduc, D. V.; Gao, D.; Leung, S.; Snider, J.; Watson, M.; Davies, S.; Bernard, P. S.; Parker, J. S.; Perou, C. M.; Ellis, M. J.; Nielsen, T. O. *J. Natl. Cancer Inst.* **2009**, *101*, 736−750.
(20) Weigelt, B.; Peterse, J. L.; Van 't Veer, L. J. *Nat. Rev. Cancer* **2005**, *5*, 591−602.
(21) O'Halloran, T.; Ahn, R.; Hankins, P.; Swindell, E.; Mazar, A. *Theranostics* **2013**, *3*, 496−506.
(22) Holohan, C.; Van Schaeybroeck, S.; Longley, D. B.; Johnston, P. G. *Nat. Rev. Cancer* **2013**, *13*, 714−726.
(23) Kulasingam, V.; Diamandis, E. P. *Nat. Clin. Pract. Oncol.* **2008**, *5*, 588−599.
(24) Moffat, J. G.; Rudolph, J.; Bailey, D. *Nat. Rev. Drug Discovery* **2014**, *13*, 588−602.
(25) Gonzalez-Suarez, E.; Jacob, A. P.; Jones, J.; Miller, R.; Roudier-Meyer, M. P.; Erwert, R.; Pinkas, J.; Branstetter, D.; Dougall, W. C. *Nature* **2010**, *468*, 103−107.
(26) Schaefer, I.; Wang, Y.; Liang, C.; Bahri, N.; Quattrone, A.; Doyle, L.; Mariño-Enríquez, A.; Lauria, A.; Zhu, M.; Debiec-Rychter, M.; Grunewald, S.; Hechtman, J. F.; Dufresne, A.; Antonescu, C. R.; Beadling, C.; Sicinska, E. T.; Rijin, M.; Demetri, G. D.; Ladanyi, M.; Corless, C. L.; Heinrich, M. C.; Raut, C. P.; Bauer, S.; Fletcher, J. A. *Nat. Commun.* **2017**, *8*, 14674.
(27) Skliris, G. P.; Parkes, A. T.; Limer, J. L.; Burdall, S. E.; Carder, P. J.; Speirs, V. *J. Pathol.* **2002**, *197*, 155−162.
(28) Neubauer, E.; Wirtz, R. M.; Kaemmerer, D.; Athelogou, M.; Schmidt, L.; Sanger, J.; Lupp, A. *Oncotarget* **2016**, *7*, 41959−41973.
(29) Wu, S. X.; Goebbels, S.; Nakamura, K.; Nakamura, K.; Kometani, K.; Minato, N.; Kaneko, T.; Nave, K.; Tamamaki, N. *Proc. Natl. Acad. Sci. U. S. A.* **2005**, *102*, 17172−17177.
(30) Richards, K. E.; Zeleniak, A. E.; Fishel, M. L.; Wu, J.; Littlepage, L. E.; Hill, R. *Oncogene* **2017**, *36*, 1770−1778.
(31) Hsia, D. A.; Tepper, C. G.; Pochampalli, M. R.; Hsia, E. Y. C.; Izumiya, C.; Huerta, S. B.; Wright, M. E.; Chen, H.; Kung, H.; Izumiya, Y. *Proc. Natl. Acad. Sci. U. S. A.* **2010**, *107*, 9671−9676.
(32) Kramer, N.; Walzl, A.; Unger, C.; Rosner, M.; Krupitza, G.; Hengstschlager, M.; Dolznig, H. *Mutat. Res., Rev. Mutat. Res.* **2013**, *752*, 10−24.
(33) Pan, W.; Zhang, T.; Yang, H.; Diao, W.; Li, N.; Tang, B. *Anal. Chem.* **2013**, *85*, 10581−10588.

DOI: 10.1021/acs.analchem.7b03146
Anal. Chem. 2017, 89, 10601−10607

(34) Yang, L.; Chen, Y.; Pan, W.; Wang, H.; Li, N.; Tang, B. *Anal. Chem.* **2017**, *89*, 6196−6201.
(35) Yang, L.; Ren, Y.; Pan, W.; Yu, Z.; Tong, L.; Li, N.; Tang, B. *Anal. Chem.* **2016**, *88*, 11886−11891.
(36) Song, S.; Liang, Z.; Zhang, J.; Wang, L.; Li, G.; Fan, C. *Angew. Chem., Int. Ed.* **2009**, *48*, 8670−8674.
(37) Song, S.; Qin, Y.; He, Y.; Huang, Q.; Fan, C.; Chen, H. *Chem. Soc. Rev.* **2010**, *39*, 4234−4243.
(38) Xu, H.; Li, Q.; Wang, L.; He, Y.; Shi, J.; Tang, B.; Fan, C. *Chem. Soc. Rev.* **2014**, *43*, 2650−2661.
(39) Luan, M.; Li, N.; Pan, W.; Yang, L.; Yu, Z.; Tang, B. *Chem. Commun.* **2017**, *53*, 356−359.
(40) Li, N.; Chang, C.; Pan, W.; Tang, B. *Angew. Chem., Int. Ed.* **2012**, *51*, 7426−7430.
(41) Ke, S. H.; Coombs, G. S.; Tachias, K.; Corey, D. R.; Madison, E. L. *J. Biol. Chem.* **1997**, *272*, 20456−20462.
(42) Pan, W.; Yang, H.; Li, N.; Tang, B. *Chem. - Eur. J.* **2015**, *21*, 6070−6073.
(43) Huang, K.; Tan, D.; Chen, K.; Walker, A. M. *Cancer Lett.* **2015**, *358*, 152−160.
(44) Paik, S.; Shak, S.; Tang, G.; Kim, C.; Baker, J.; Cronin, M.; Baehner, F. L.; Walker, M. G.; Watson, D.; Park, T.; Hiller, W.; Fisher, E. R.; Wickerham, D. L.; Bryant, J.; Wolmark, N. *N. Engl. J. Med.* **2004**, *351*, 2817−2826.
(45) Charpentier, M. S.; Whipple, R. A.; Vitolo, M. I.; Boggs, A. E.; Slovic, J.; Thompson, K. N.; Bhandary, L.; Martin, S. S. *Cancer Res.* **2014**, *74*, 1250−1260.

DOI: 10.1021/acs.analchem.7b03146
Anal. Chem. 2017, 89, 10601−10607